Single-mode GaAs/AlGaAs quantum cascade microlasers*

Gao Yu(高瑜), Liu Junqi(刘俊岐), Liu Fengqi(刘峰奇)†, Zhang Wei(张伟), Zhang Quande(张全德), Liu Wanfeng(刘万峰), Li Lu(李路), Wang Lijun(王利军), and Wang Zhanguo(王占国)

(Key Laboratory of Semiconductor Materials Science, Institute of Semiconductors, Chinese Academy of Sciences, Beijing 100083, China)

Abstract: Single-mode edge emitting GaAs/AlGaAs quantum cascade microlasers at a wavelength of about 11.4 μm were realized by shortening the Fabry-Pérot cavity length. The spacing of the longitudinal resonator modes is inversely proportional to the cavity length. Stable single-mode emission with a side mode suppression ratio of about 19 dB at 85 K for a 150-μm-long device was demonstrated.

Key words: quantum cascade lasers; GaAs/AlGaAs; single-mode emission; short cavity length

DOI: 10.1088/1674-4926/30/11/114007 **EEACC:** 2520

1. Introduction

The quantum cascade laser (QCL) is one of the most promising light sources for mid- and far-infrared ranges. QCLs have wide applications in areas such as industrial process control, medical diagnostics, free space communications, and remote chemical sensing[1−3]. In practical applications of QCLs, stable and single-mode emissions are required in most situations. To meet these needs, structures such as distributed feedback gratings, micro cavity resonators and deeply etched Bragg mirrors have been employed[4−7]. These techniques, however, make the fabrication process of single-mode QCLs very complicated and less controllable.

It is known that with a decrease of cavity length, the spacing of the Fabry-Pérot (F-P) modes increases, which would reduce the allowed oscillation modes in the limited gain bandwidth of QCLs. When the secondary modes beside the master mode pass over the range of gain band-width, only the master mode acquires sufficient gain to reach its threshold. This makes a short F-P cavity a simple structure for QCLs to get single-mode emission. Based on this idea, single-mode InP-based short cavity QCLs have been demonstrated with wavelengths of $\lambda \approx 5.47$ μm and $\lambda \approx 7.84$ μm[8].

Although the InP-based QCLs have superior properties due to the higher electronic confinement in the conduction band, GaAs-based QCLs have higher flexibility in processing, in structure design, and the potential for commercialization on a larger scale. In this paper, we report on short cavity edge emitting GaAs/AlGaAs quantum cascade microlasers operating at a wavelength of about 11.4 μm. For a 150-μm-long microlaser, single-mode operation with a side mode suppression ratio of 19 dB at 85 K is achieved.

2. Fabrication and measurement

The QCL structure demonstrated in this paper was grown by solid source molecular beam epitaxy (MBE) on n-doped (Si, 2×10^{18} cm^{-3}) GaAs substrate in a single growth step. The active region was based on the so-called four-quantum-well active region[9]. The growth started with a 1 μm highly doped (Si, 6–8 $\times 10^{18}$ cm^{-3}) GaAs waveguide layer, followed by the waveguide core which consists of 40 stages of injector/active regions (~2 μm thick) and was sandwiched between two layers of 3.5 μm low-doped (Si, 4×10^{16} cm^{-3}) GaAs cladding material. Finally, a 1 μm highly doped (Si, 6–8 $\times 10^{18}$ cm^{-3}) GaAs layer was grown as the top cladding and contact layer. Figure 1 shows the layer sequence of the waveguide. The layer sequence of one period, in nanometers, starting from the injection barrier is 5.1/**2.0**/0.85/**5.7**/0.85/**5.1**/0.85/**4.8**/2.8/**3.7**/1.7/**3.1**/1.7/**2.8**/2.0/**3.1**/2.6/**3.1,** where GaAs parts are in bold, $Al_{0.45}Ga_{0.55}As$ in roman, and n-doped layers (Si, 6.5×10^{17} cm^{-3}) are underlined. The emission wavelength of the QCL is determined by the conduction band discontinuity ΔE_c between the two materials of the active region, and can be tailored by varying the thickness or the composition of the quantum well/barrier[3,9].

An X-ray diffraction spectrum for the waveguide core is illustrated in Fig. 2. The satellite peaks have a full width at half maximum (FWHM) of about 1 arcsec, indicating good material quality. The diffraction simulation is also shown in

GaAs	1 μm	6–8 $\times 10^{18}$ cm^{-3}
GaAs	3.5 μm	4×10^{16} cm^{-3}
Active+Injector	$\times 40$	
GaAs	3.5 μm	4×10^{16} cm^{-3}
GaAs	1 μm	6–8 $\times 10^{18}$ cm^{-3}
GaAs Substrate		2×10^{18} cm^{-3}

Fig. 1. Schematic cross section of the complete GaAs/AlGaAs laser structure grown by MBE.

* Project supported by the National Research Projects of China (Nos. 60525406, 60736031, 60806018, 60906026, 2006CB604903, 2007AA03Z446, 2009AA03Z403).

† Corresponding author. Email: fqliu@red.semi.ac.cn

Received 29 April 2009, revised manuscript received 2 June 2009

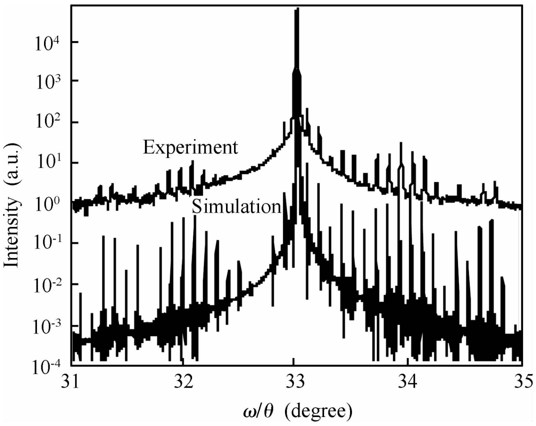

Fig. 2. Experimental and simulated X-ray diffraction of a 40 period GaAs/AlGaAs QCL.

Fig. 2. The two spectra are nearly identical, indicating that the layer thicknesses, material compositions, and interfaces are well controlled and very uniform throughout the 40-period structure.

A simple process was adopted in the fabrication. The wafer was processed by conventional photolithography and wet chemical etching in a $H_2SO_4 : H_2O_2 : H_2O = 5 : 1 : 1$ solution to form a double-channel ridge structure with a ridge width of 46 μm and a channel depth penetrating through the waveguide core. A 300-nm-thick SiO_2 layer was then deposited by chemical vapor deposition for insulation around the ridges. A 25 μm window was opened on top of the ridge for current injection. A non-alloyed Ti/Au (20/150 nm) ohmic contact was evaporated to the top layer. After the wafer was thinned down to about 100 μm, an alloyed AuGeNi/Au (100/150 nm) contact was evaporated on the backside. The samples were cleaved manually into bars with different lengths. Both uncoated and high-reflectivity (HR) coated devices were fabricated. The HR coating consists of Al_2O_3/Ti/Au/Al_2O_3 (200/10/80/100 nm) deposited on the back mirror facet by electron beam evaporation. The lasers were bonded epilayer-down on copper submounts with In solder.

For characterization, the submounts were placed on a temperature-controlled cold finger in an evacuated liquid nitrogen cryostat. The spectral measurements were carried out with a Fourier transform infrared (FTIR) spectrometer in step-scan mode. The optical output power emitted from the front facet of the laser was measured with a thermopile detector placed directly near the window of the cryostat. The output power is not corrected by the transmission of the optics windows (BaF_2, the transmission efficiency is about 90% for a wavelength of about 11 μm) and the collection efficiency of the detector is about 60%. The collection efficiency is limited by the distance between cryostat and detector, and the far-field distribution of the laser. The estimated value is about 60%.

3. Device performance

Figure 3 shows scanning electron microscopy (SEM) images of the epilayer-down bonded laser with a cavity length of

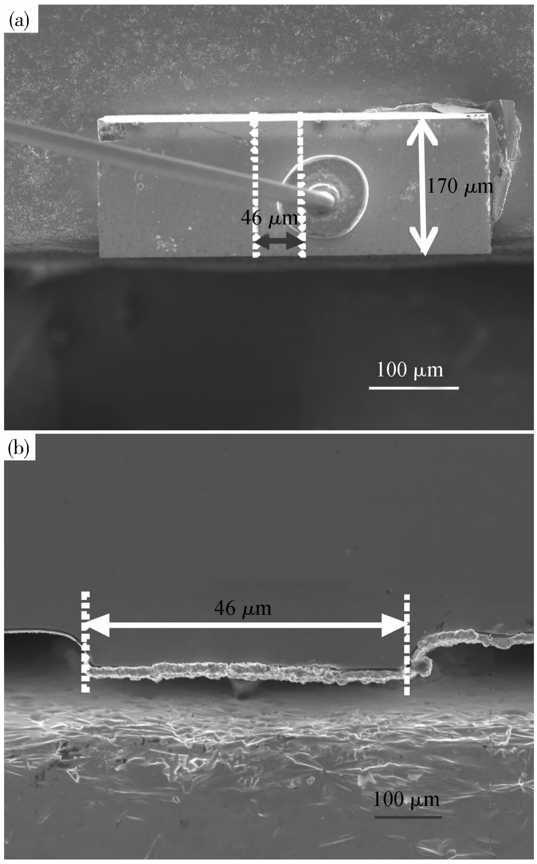

Fig. 3. (a) SEM image of the 170-μm-long QCL with the ridge region indicated; (b) Cross-sectional SEM image of the 170-μm-long QCL.

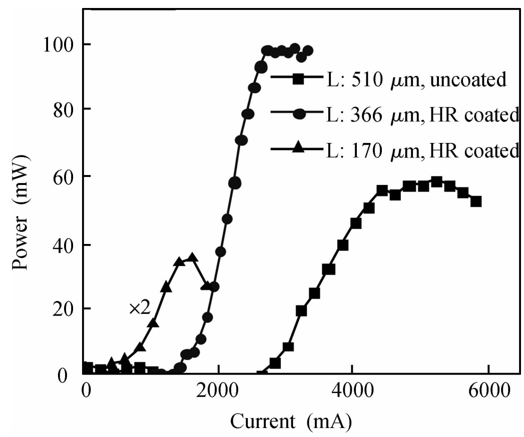

Fig. 4. Light–current (*L–I*) characteristics of QCLs with different back facet conditions (uncoated and HR coated) and different cavity lengths (170, 366 and 510 μm, respectively). Measurements were performed at 85 K in pulsed mode (5 μs, 1 kHz).

170 μm and a ridge width of 46 μm. Figure 3(b) shows a cross-section SEM image of Fig. 3(a).

Figure 4 shows the light–current curves of three 46 μm-wide QCLs with cavity lengths of 170, 366 and 510μm at 85 K. The measurements were carried out with a duty cycle of 0.5% (5 μs, 1 kHz). The QCLs with cavity lengths of 170 and 366 μm have HR coatings at the back facet and the 510-μm-long one is uncoated. The maximum powers are 17.3, 97.5 and 58.3 mW and the corresponding threshold current densities are 7.0, 9.4 and 11.4 kA/cm^2 for the QCLs with cavity lengths of 170, 366 and 510 μm, respectively. The 366-μm-long and

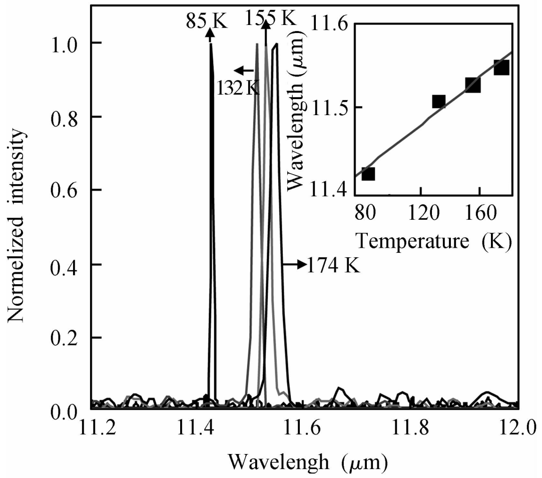

Fig. 5. Pulsed lasing spectra (1 μs, 1 kHz) of a 46-μm-wide and 366 μm-long QCL for temperatures between 85 and 174 K. The inset shows the linear tuning of the wavelength with temperature.

170-μm-long QCLs with HR coatings have relatively lower threshold current densities than the uncoated 510-μm-long laser, because the mirror loss is reduced by the HR coatings.

Typically, QCLs with cleaved facets have low facet reflectivity $R_1 = R_2 = 0.28$. The mental-on-insulator coatings can provide a much higher reflectivity (close to 99%). The mirror loss $\alpha_m = \frac{1}{2L} \ln \frac{1}{R_1 R_2}$, where L is the cavity length and R_1 and R_2 are the reflectivities of two facets. The α_m values for the 170-μm-long and 366-μm-long with HR coatings and 510-μm-long uncoated microlasers are 37.4, 17.4 and 25.0 cm^{-1}, respectively. Compared to the 366-μm-long QCL, the threshold current density of the 170-μm-long QCL is lower, which is unusual and is attributed to the higher heat removal efficiency.

Figure 5 shows lasing spectra at temperatures between 85 and 174 K for a 366-μm-long QCL. The inset of the figure shows that the emission wavelengths redshift with temperature and the data can be fitted by a linear function. The spectra were measured with the same pulse frequency and duty cycle (1 kHz and 0.1% duty cycle) at about $1.1I_{th}$ of each QCL. As can be seen from the figure, the 366-μm-long QCL shows stable single-mode emission within the temperature range. The peak wavelength is tuned from 11.43 μm at 85 K to 11.55 μm at 174 K linearly with a wavelength-temperature tuning coefficient $d\lambda/dT = 1.35$ nm/K.

Figure 6 shows lasing spectra of QC microlasers with cavity lengths of 150, 170 and 366 μm measured at 85 K. The measurements were conducted in pulsed mode with a duty cycle of 0.1% (1 μs, 1 kHz). As can be seen from the figure, all three devices show single-mode operation without any detectable side modes. The variation of the wavelengths with the different cavity lengths is mainly caused by the different mode indices and the narrow gain spectra[10]. The side mode suppression ratios (SMSR) are about 13, 15 and 19 dB for the microlasers with cavity lengths of 366 μm, 170 μm and 150 μm, respectively. For the 150-μm-long laser, the SMSR is only slightly smaller than the SMSR of the short cavity GaAs-based QCL with deeply etched Bragg mirrors as reported in Ref. [6]. This demonstrates the effectiveness of the short cavity alone

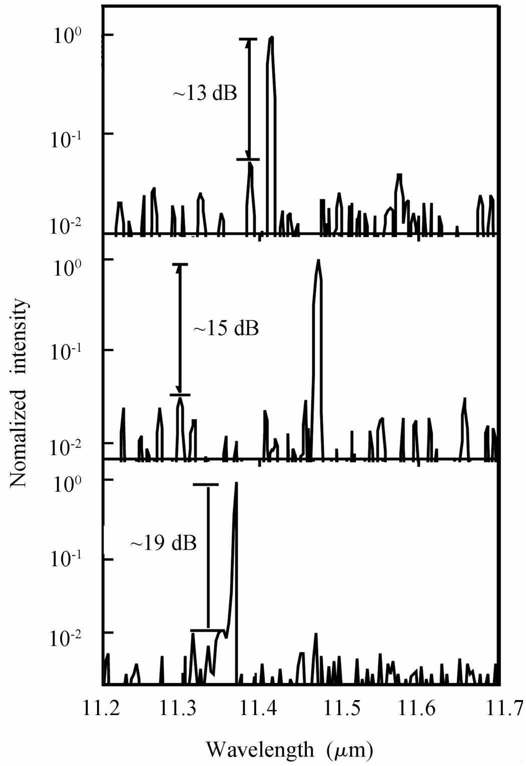

Fig. 6. Single-mode spectra of microlasers with cavity lengths of 150, 170 and 366 μm at 85 K, measured in pulsed mode (1 μs, 1 kHz).

as a simple route to obtain single-mode emission of QCLs.

The longitudinal mode spacing of the F-P QCL is given by $\Delta\nu_{long} = 1/2n_g L$, where L is the cavity length and n_g is the group refractive index of the material. For the QCLs studied in this paper, n_g is about 3.3 and the calculated mode spacing of the 150-μm-long laser is as large as 10.1 cm^{-1}. So the allowed oscillation modes of the QCL are few. As the secondary modes beside the master mode pass over the range of gain band-width, only the master mode acquires sufficient gain to reach its threshold.

4. Conclusion

In conclusion, we have fabricated short cavity single-mode GaAs/AlGaAs QC microlasers at a wavelength of 11.4 μm. The single-mode operations of 366-μm, 170-μm-long microlasers have peak optical powers of 97.5, 17.3 mW at 85 K. The 150-μm-long microlaser exhibits pronounced single-mode operation with a side mode suppression ratio of about 19 dB at 85 K. This demonstrates the effectiveness of the short cavity alone as a simple route to obtain single-mode emission of QCLs.

Acknowledgements

The authors would like to acknowledge Liang Ping, Hu Ying, and Sun Hong for their help with device fabrication.

References

[1] Li Lu, Liu Fengqi, Shao Ye, et al. Low-threshold high-temperature operation of λ ~7.4 μm quantum cascade lasers.

Chin Phys Lett, 2007, 24(6): 1577
[2] Evans A, Yu J S, David J, et al. High-temperature, high-power, continuous-wave operation of buried heterostructure quantum-cascade lasers. Appl Phys Lett, 2004, 84(3): 314
[3] Faist J, Capasso F, Sivco D L, et al. Quantum cascade lasers. Science, 1994, 264: 553
[4] Guo Yu, Liu Fengqi, Liu Junqi, et al. Second-order distributed feedback quantum cascade lasers at 7.8 μm. Chinese Journal of Semiconductors, 2005, 26(3): 627
[5] Gianordoli S, Hvozdara L, Strasser G, et al. Long-wavelength (λ = 10 μm) quadrupolar-shaped GaAs-AlGaAs microlasers. IEEE J Quantum Electron, 2000, 36(4): 458
[6] Höfling S, Bazhenov A, Fischer M, et al. GaAs/AlGaAs quantum cascade micro lasers based on monolithic semiconductor-air Bragg mirrors. Electron Lett, 2004, 40(2): 120
[7] Semmel J, Nähle L, Höfling S, et al. Edge emitting quantum cascade microlasers on InP with deeply etched one-dimensional photonic crystals. Appl Phys Lett, 2007, 91: 071104
[8] Liu Fengqi, Guo Yu, Li Lu, et al. Single mode operation of short-cavity quantum cascade lasers. Chinese Journal of Semiconductors, 2006, 27: 679
[9] Liu Junqi, Li Lu, Liu Fengqi, et al. GaAs/AlGaAs quantum cascade lasers with double-resonant-phonon depopulation. Chin Semicond Technol, 2008, 33(Suppl): 59
[10] Höfling S, Reithmaier J P, Forchel A. Device performance and wavelength tuning behavior of ultra-short quantum-cascade microlasers with deeply etched bragg-mirrors. IEEE J Sel Topics Quantum Electron, 2005, 11: 1048